

UCLA

UCLA Electronic Theses and Dissertations

Title

Pulmonary Hypertension in Rats is Associated with Vascular Remodeling and Neuro-inflammation in the Brain

Permalink

<https://escholarship.org/uc/item/9vq1w873>

Author

Sarji, Shervin

Publication Date

2018

Peer reviewed|Thesis/dissertation

UNIVERSITY OF CALIFORNIA

Los Angeles

Pulmonary Hypertension in Rats is Associated with Vascular
Remodeling and Neuroinflammation in the Brain

A thesis submitted in partial satisfaction
of the requirements for the degree Master of Science
in Physiological Science

by

Shervin Sarji

2018

© Copyright by

Shervin Sarji

2018

ABSTRACT OF THE THESIS

Pulmonary Hypertension in Rats is Associated with Vascular Remodeling and Neuroinflammation in the Brain

by

Shervin Sarji

Master of Science in Physiological Science

University of California, Los Angeles, 2018

Professor Arthur P. Arnold, Chair

Pulmonary arterial hypertension (PAH) is a chronic pulmonary vascular disease characterized by increased pulmonary vascular resistance. Recent studies implicate sympathetic overactivation in PAH and demonstrate that PAH patients suffer from cognitive impairments, depression, anxiety, and decreased quality of life which indicate severe neuropathology. Neuropathology of PAH remains understudied yet may produce additional insights into the pathogenesis of this devastating disease. Thus, we compared a clinically relevant rat model of experimental pulmonary hypertension (PH) with available post-mortem human data using histological methods to study changes associated with PAH in the brain. We found in rats and humans that PAH is associated with vascular wall thickening of brain parenchymal arterioles and gliosis with non-ischemic pathology. Furthermore, we found evidence for neuroinflammation surrounding brain parenchymal arterioles in experimental PH rats.

The thesis of Shervin Sarji is approved.

Mansoureh Eghbali

Fernando Gomez-Pinilla

Arthur P. Arnold, Committee Chair

University of California, Los Angeles

2018

Table of Contents

List of Acronyms.....	v
Acknowledgements.....	vi
Introduction.....	1
Methods	
Animal Model of Severe PH.....	3
Cardiopulmonary Hemodynamics to Assess Disease Progression.....	3
Gross Histological Evaluation of the Heart.....	4
Histopathologic Analysis and Imaging of Lungs with Trichrome.....	4
H&E Staining and Assessment of Brain Arterioles.....	4
Immunohistochemistry Staining and Assessment of Gliosis.....	5
Immunofluorescence Staining and Assessment of Neuroinflammation.....	6
Assessment of Post-Mortem Human Brain Tissue	7
Results	
Development of Severe Angioproliferative PH in Rats.....	8
PH is Associated with Vascular Wall Thickening in Brain Arterioles.....	8
PH is Associated with Neuroinflammation.....	9
PH is not Associated with Severe Gliosis.....	9
Discussion.....	10
Figure 1.....	14
Figure 2.....	15
Figure 3.....	16
Figure 4.....	17
Figure 5.....	17

List of Acronyms

Pulmonary arterial hypertension (PAH)

Central nervous system (CNS)

Autonomic nervous system (ANS)

Renin-angiotensin-aldosterone system (RAAS)

Pulmonary Hypertension (PH)

Macrophage Inflammatory Protein-1 (or MIP-1 α , also known as CCL3)

Multiple sclerosis (MS)

Glial fibrillary acidic protein (GFAP)

Vascular endothelial growth factor receptor (VEGF-R)

Right ventricular systolic pressures (RVSP)

Right Ventricle (RV)

Left Ventricle (LV)

Interventricular septum (IVS)

3,3'-Diaminobenzidine (DAB)

Tumor necrosis factor alpha (TNF- α)

Experimental autoimmune encephalomyelitis (EAE)

Circumventricular Organ (CVO)

Angiotensin-II receptor type 1 (AT1R)

Monocrotaline (MCT)

ACKNOWLEDGEMENTS

I would first like to thank Dr. Eghbali, my P.I., for seeing something in me that I could not have seen myself when I first started in her lab, and for continuously challenging me to strive for greater heights in my own life and in my research. Her dedication and patience with those she takes under her wing is both admirable and contagious; and is something I will take with me for the rest of my life in striving to provide a better future for myself and those around me. I would also like to thank Dr. Khanlou, who taught me the ins and outs of clinical neuropathology – and more than anything, provided provocative conversations and insights into the clinical world and my future in medicine. Similarly, I would like to thank Dr. Umar for answering my endless questions about translational research, training in pulmonary hypertension research, and indulging my ideas for my project. I want to thank Dr. Ruffenach especially for the constant input and his sincerity in sharing with me the realities of research my successes in research. I would also like to thank my committee members, Dr. Arnold and Dr. Gomez-Pinilla. The class discussions concerning the effects of peripheral systems on the central nervous system were catalyst to developing concepts for my project. To start a project on an especially novel concept is a daunting task for all those involved. For that, I would like to thank the several brave undergraduate students who helped along the way, and to Mylenne for sharing with me this journey of studying neuroinflammation in pulmonary hypertension. Finally, I would like to thank Shayan Moazeni for pushing me to consider a future in research in the first place. Before we knew it, we were changing the hearts and minds of more established researchers in the field of pulmonary hypertension to consider new avenues and new ideas for researching this devastating disease – which is more than I ever could have imagined we would accomplish during our time in college. You have all given me the tools necessary to realize my dreams, and the courage to pursue them. Thank you.

Pulmonary Hypertension in Rats is Associated with Vascular Remodeling and Neuro-inflammation in the Brain

Shervin Sarji, BS, Negar Khanlou, MD*, Gregoire Ruffenach, PhD, Shayan Moazeni, BS, Ali Said, B.S., Crystal Eshraghi, B.S., Christine Cunningham, B.S., Soban Umar, MD, PhD, Mansoureh Eghbali, PhD

Department of Anesthesiology and Perioperative Medicine, David Geffen School of Medicine at UCLA, Los Angeles, CA, USA

*Department of Pathology, David Geffen School of Medicine at UCLA, Los Angeles, CA, USA

Correspondence:

Dr. Mansoureh Eghbali

Department of Anesthesiology, Division of Molecular Medicine

David Geffen School of Medicine at UCLA

BH-160 CHS, 650 Charles E Young Dr. South,

Los Angeles, CA 90095-7115

Phone: (310) 206-0345

E-mail: meghbali@ucla.edu

Key words: Pulmonary hypertension, vascular remodeling, neuro-inflammation, brain

Introduction

Pulmonary arterial hypertension (PAH) is a chronic pulmonary vascular disease characterized by increased pulmonary vascular resistance (1) . The pathogenesis of PAH is not fully understood although it is a complex multifactorial disease. The central nervous system (CNS) is the master regulator for the cardiopulmonary system involved in the regulation of the autonomic nervous system (ANS) and renin-angiotensin-aldosterone system (RAAS) already demonstrated to be involved in PAH pathogenesis. Furthermore, recent studies also implicate sympathetic overactivation in PAH (2,3) and demonstrated that PAH patient suffer from cognitive impairments, depression, anxiety, and decreased quality of life (4) which indicate severe neuropathology. Neuropathology of PAH remains understudied yet may produce additional insights into this the pathogenesis of this devastating disease.

Until recently the CNS was considered to be immunologically inert and anatomically isolated from the peripheral immune system, though this is no longer the consensus in this field of study and immune-privilege varies at the very least with age and brain location (5,6). The effects of peripheral inflammation on the CNS have been discussed in literature like those linking peripheral infections to depression (7) and systemic inflammation to neurodegeneration (8). In the lungs, literature has touched on possible mechanisms in lung inflammatory diseases which may adversely affect autonomic or hormonal regulation (9) and have explored PAH treatments used in research which may affect the ANS (10). In monocrotaline (MCT) induced PH rats, upregulated inflammatory, sympathetic, and RAAS pathogenic factors are implicated in the development of the disease (11) in part by inducing neuroinflammation in the paraventricular nucleus (PVN), increasing sympathetic drive; and attenuation of PH pathology with intracerebroventricular infusion minocycline (12). However, it is still unclear whether PAH exhibits the neuropathology required to induce both sympathetic and cognitive changes which have been observed mostly in other contexts.

Neuroinflammation, or inflammation in the brain, is generally considered to be a chronic condition which can be a result of disease or contribute to disease progression. Glial cells, namely microglia and astrocytes, are important players for regulating neuroinflammatory processes and express an assortment of cytokines and chemokines in response to mild to severe insults to the nervous system. Glial expression of chemokine Macrophage Inflammatory Protein-1 (or MIP-1 α , also known as CCL3) is a well-studied neuroinflammatory marker involved with remyelinating processes in the CNS, is associated with cognitive deficits when overexpressed, and is expressed in severe neurological diseases like demyelinating multiple sclerosis (MS) (13) as well as in relatively less inflammatory diseases like atherosclerosis (14). One study on atherosclerotic mice showed mice exhibited thicker brain arterioles, increased perivascular CCL3 expression, and associated cognitive deficits (14). Astrocytes form glial scars and express GFAP in response to trauma, infection, ischemia, hypoxia, blood-brain barrier damage, inflammation, and oxidative stress, which in turn affect axon regeneration and neurological recovery (15,16). The reactive nature of glial cells which facilitate neuroinflammation allows some inferences to be made of central regulatory mechanisms in response to PAH.

Here we investigated whether brain vascular remodeling is part of the histopathological presentation of PAH by vascular wall thickening in brain parenchymal arterioles and neuroinflammation of parenchymal cells in close proximity to brain arterioles, which could participate in RAAS or ANS dysregulation seen in PAH. Thus, comparing a clinically relevant rat model of angio-proliferative PH and available post-mortem human data to study changes associated with PH in the brain.

Methods

Animal Model of Severe PH

PH was induced in male Sprague Dawley rats (200-250g) by a single intraperitoneal injection of vascular endothelial growth factor receptor (VEGF-R) inhibitor, Sugen5416 (SU/HY, 20mg/kg), followed by 3 weeks of hypoxia (10% O₂) and then 2 weeks of normoxia (n=5) exposure. Saline treated normoxic rats served as controls (n=5).

Cardiopulmonary Hemodynamics to Assess Disease Progression

Serial transthoracic echocardiography was performed to monitor disease progression. VisualSonics Vevo 2100 echocardiogram device with a 30-MHz linear transducer was used to perform the B-mode and pulmonary pulsed-wave Doppler echocardiography of PA flow. The probe was placed in a parasternal long-axis position to visualize the PA outflow tract. Pulsed flow Doppler imaging was then overlaid to observe the dynamics of blood flow through the PA valve (Vevo 2100 version: 1.5.0). Direct cardiac catheterization was performed terminally to assess cardiopulmonary hemodynamics. Right ventricular systolic pressures (RVSP, mmHg) were measured terminally by direct RV catheterization to assess PH by inserting a catheter into the RV immediately prior to sacrifice. Briefly, the rats were anesthetized with a mixture of Ketamine (80 mg/kg) and Xylazine (8 mg/kg) administered *via* intraperitoneal injection. The animals were placed on a controlled warming pad to keep the body temperature constant at 37°C. After a tracheostomy was performed, a cannula was inserted, and the animals were mechanically ventilated using a rodent ventilator (Harvard Apparatus, Canada). Rats were placed under a stereomicroscope (Zeiss, Hamburg, Germany), and a pressure-conductance catheter (model 1.4F Millar SPR-671) was introduced *via* the apex into the RV and positioned towards the pulmonary valve. The catheter was connected to a pressure transducer (Power Lab, ADInstruments) and RV pressures were

recorded digitally. After recording the RVSP, heart and lungs were removed rapidly under deep anesthesia for preservation of protein integrity.

Gross Histological Evaluation of the Heart

The RV wall, the left ventricular (LV) wall, and the interventricular septum (IVS) were dissected, and the ratio of the RV to LV plus septum weight [$RV/(LV + IVS)$] was calculated as an index of RV hypertrophy. Student's T-test was used to test for statistical significance. Values were expressed as mean \pm SEM.

Histopathologic Analysis and Imaging of Lungs with Trichrome

Lungs were first weighed, perfused, then fixed for further histological investigation. Briefly, whole lungs were isolated and inflated manually using a syringe by perfusing 4% paraformaldehyde in 0.1 M Na₂HPO₄ and 23 mM NaH₂PO₄ (pH 7.4) through the trachea. Isolated perfused lungs were fixed in 4% paraformaldehyde at 4°C overnight. Following fixation, the tissue was immersed in 20% sucrose at 4°C overnight and embedded using optimum cutting temperature compound for cryostat sectioning. Five μ m thick lung tissue sections were obtained with a cryostat at -20°C (Microm HM525, Thermo Scientific). Standard Masson Trichrome (Sigma) staining was performed according to the manufacturer's protocol, and images were acquired using a confocal microscope with bright field (Nikon).

H&E Staining and Assessment of Brain Arterioles

Coronal sections were obtained from anterior and posterior brain regions (bregma 1.8mm to .8mm and bregma -1mm to -5mm) to assess vascular pathology of brain parenchymal arterioles in rodents. Sections were hematoxylin/eosin (H&E) staining was performed according to manufacturer's protocol. Images used for quantification were acquired at 40x magnification using

a confocal microscope with bright field (Nikon). Arteriole wall thickness was measured as lumen size over total vessel size for all identified arterioles (<50 μm) within cortical and non-cortical regions of each coronal section; totaling 83 arterioles for the control group (n=3) and 81 arterioles for the PAH group (n=5). Values were expressed as mean \pm SEM. To compare more than 2 groups, we used one-way ANOVA followed by a Dunnett's multiple comparison test to compare individual means with a control mean or a Sidak multiple comparisons test to compare a set of means. Furthermore, the normality was verified using the Shapiro-Wilk test and the Brown-Forsythe (Modified Levene test) test was used to verify homogeneity of variances. For some variables, when these assumptions were not fulfilled, values were log transformed to stabilize variances and statistical analyses were performed on these log transformations. Correlation analyses were made by Pearson correlations. A significance level inferior to 5% ($p < 0.05$) was considered statistically significant. All analyses were made with Graph Pad Prim v.6 software. Total blood parenchymal arterioles in anterior and posterior regions were counted and tested for significance using students t-test. Values were expressed as mean \pm SEM of vascular wall thickness determined by wall to lumen ratio. Additionally, anterior and posterior brain sections were assessed for vascular density. Brain parenchymal arterioles were counted from anterior and posterior sections and combined for each group. Values represent mean \pm SEM number of total arterioles.

Immunohistochemistry Staining and Assessment of Gliosis

To stain reactive astrocytes expression GFAP for quantification, Horseradish peroxidase (HRP) staining was carried out on rodent coronal sections (10 μm) within a similar area (bregma -1mm to -5mm). Primary antibody Glial fibrillary acidic protein (GFAP) was first used, followed by secondary antibody HRP anti-GFAP, then 3,3'-Diaminobenzidine (DAB) peroxidase staining protocol was followed using kit manufacturers protocol. Sections were then dipped in hematoxylin

for 30 seconds to visualize tissue not expressing GFAP. Images were obtained by UCLA's Department of Neuropathology using Scanscope. Images were evaluated with Aperio Imagescope (v12.3.2.8013) separately and in accordance with clinical protocols. Positive Pixel Count Algorithm v9 was first tested by adjusting hues and color detection for GFAP-HRP positive pixels (Brown) and non-GFAP pixels (Blue) and was accurate without change which was consistent with methods used by neuropathology. The area selected for pixel count was carried out manually and contained the whole coronal section on each slide for control and PAH rats, omitting naturally occurring gaps formed by lateral ventricles and irregularities formed during tissue collection or during the staining process. Areas evaluated averaged to 44mm² for both control group (n=5) and PAH group (n=5). Reported values represent number of GFAP positive pixels over number of total pixels (Positivity = NPositive/NTotal), where NPositive is total positive pixels, and NTotal is the total negative pixels and positive pixels.

Immunofluorescence Staining and Assessment of Neuroinflammation

Coronal sections (10 µm) containing the anterior hypothalamus were used to assess neuroinflammation using immunofluorescence staining in control (n=5) and PAH (n=5) rats. Sections were washed with PBS+0.1% Triton three times and incubated with 5% normal donkey serum in PBS+0.1% Triton for 30 minutes to reduce un-specific binding of primary anti-bodies and background. Following blocking, the sections were incubated with primary antibodies against α -smooth muscle actin (α -SMA 1:500) and CCL3/MIP1- α (1:25) in PBS+0.1% Triton+1% normal donkey serum for one hour at 37°C. Sections were then washed with PBS+0.1% Triton three times, incubated with the appropriate secondary antibodies (1:1000) in PBS+0.1% Triton+1% normal donkey serum at room temperature for one hour. After washing the secondary antibodies with PBS+0.1% Triton three times, the sections were incubated with DAPI and then mounted for imaging using Prolong gold (Molecular Probes). Fluorescent images were acquired with a

confocal microscope (Nikon) at 40x magnification and used for quantification. α -SMA fluorescence was used to localize brain arterioles, DAPI for nuclei, and MIP-1 α /CCL3 to indicate inflammatory positive cells. Total cells (determined by DAPI alone) and MIP-1 α /CCL3 positive cells (determined by MIP-1 α /CCL3 and DAPI co-staining) were counted within a 150 μ m radius circle area around each arteriole. Only nonvascular cells were considered. Data is presented as the mean percentage of MIP-1 α /CCL3 positive cells per group \pm SEM.

Assessment of Post-Mortem Human Brain Tissue

H&E stained slides from five post-mortem patients with PH were qualitatively evaluated by a neuropathologist and compared to PH rats. Slides were evaluated for possible glial, vascular, and ischemic changes.

Results

Development of Severe Angioproliferative PH in Rats

Rats treated with a single injection of VEGF-R antagonist SU5416 (Sugen) followed by 3 weeks of hypoxia and 2 weeks of normoxia treatment (Figure 1) developed severe pulmonary hypertension with significantly higher RVSPs in SU/HY group compared to control [81.2 ± 14.2 mmHg vs. 30.3 ± 2.7 mmHg; $p=0.015$], confirming the development of severe PH (Figure 2A). SU/HY rats also developed severe RV hypertrophy as evidenced by significantly increased RV hypertrophy index (Fulton index) [0.62 ± 0.09 vs. 0.28 ± 0.09 ; $p=0.004$] (Figure 2B). SU/HY rats demonstrated significantly higher lung weights compared to controls, most likely from increased remodeling in their lungs [2.1 ± 0.14 vs. 1.59 ± 0.07 g; $p=0.013$] (Figure 2C). Severe PH in SU/HY rats was also associated with RV hypertrophy and dilatation as seen with B-mode echocardiography and echocardiographic evidence of PH on PA pulsed-wave Doppler showing mid-systolic notching (Figure 2D). SU/HY rat lungs also demonstrated severe pulmonary vascular remodeling compared to controls (Figure 2E).

PH is Associated with Vascular Wall Thickening in Brain Arterioles

ANOVA revealed brain parenchymal arteriole wall thickness was significantly different with between PH rats and control with no interaction between all compared regions (Figure 3), indicating PH rats had on average thicker arterioles throughout the cerebrum. Compared to control rats, PH rats exhibited significantly less brain parenchymal arterioles in the anterior region [15.7 ± 3.2 vs. 8.4 ± 0.7 arterioles; $p=0.027$], but not the posterior region [12.0 ± 2.5 vs. 7.8 ± 1.2 arterioles; $p=0.130$]. When all arterioles in both regions were considered, PH group exhibited significantly less arterioles than control [27.7 ± 4.2 vs. 16.2 ± 1.8 ; $p=0.025$]. Of the five PAH patients examined, only 2 exhibited non-vascular pathology.

PH is Associated with Neuroinflammation

To assess for neuro-inflammation and microglia activation in the brain, immunofluorescence staining of brain sections was performed with MIP-1 α (CCL3), smooth muscle actin (blood vessels) and DAPI (nuclei) on rodent sections. Brain arterioles of PH rats were associated with a significantly greater percentage of MIP-1 α (CCL3) positive non-vascular cells compared to control [30.9% \pm 4.7 vs. 15.2% \pm 4.4; $p=0.0006$] (Figure 4).

PH is not Associated with Severe Gliosis

GFAP expression was measured using clinically relevant methods to determine degree of gliosis in rodent brain sections. Positive Pixel Count of GFAP antibody staining revealed no statistical difference between control and rats with PH [0.056 \pm 0.018 vs 0.076 \pm 0.008; $p=0.36$] (Figure 5). GFAP stained sections for rodents were compared to available H&E stained sections for humans. Mild gliosis and white matter damage with no definite ischemic neural pathology were seen in PH rats as well as in post-mortem PH patient brain sections.

Discussion

The present study demonstrates for the first time that severe PH in rats is associated with structural changes to brain parenchymal arterioles and increased pro-inflammatory expression of CCL3 in brain parenchymal cells surrounding arterioles.

Rats treated with SU/HY exhibited severe PH pathology (Figure 2), significantly thicker brain arterioles in all evaluated regions (Figure 3B), and overall less arterioles in total (Figure 3C). Furthermore, we found similar histological changes in human brain vasculature, noting that microvascular hyalinization and vascular wall thickening were consistent between rat and human samples with PAH.

Our data demonstrating increased vascular thickness in humans and the animal model of PH are in agreement with the decreased cerebrovascular perfusion seen in PAH (17). Reduced cerebrovascular perfusion may be a result of structural vascular changes in brain parenchymal arterioles shown in our study in addition to enhanced chemoreflex sensitivity and CO₂ accumulation in the cerebrospinal fluid shown in Malenfant et al's study on PAH patients. Interestingly, we found that anterior, but not posterior regions had significantly less brain arterioles in rats with PH (data not shown). In PAH patients, impaired executive function such as decision making, mental processing speeds, and social functioning (4) can be the result of decreased frontal brain perfusion as shown in patients with asymptomatic carotid stenosis (18). Nonetheless, anatomical limitations are presented to differentiate between regions supplied by the internal carotid and vertebral arteries which would respectively supply the ventral-anterior and dorsal-posterior cerebrum with some overlap (19,20).

The purpose of evaluating gliosis in our study was meant to determine if inflammation was prevalent throughout the brain which could indicate chronic hypoxia or severe inflammation in the CNS. Indeed, astrocytes form glial scars express GFAP in response to trauma, infection, ischemia or hypoxia, blood-brain barrier damage, inflammation, and oxidative stress; which in

turn affect axon regeneration and neurological recovery (15,16). It is likely that generalized gliosis in both human and rats has a small or negligible effect since pathological assessment revealed mild gliosis, and because gliosis was not discernable in PH rats after analysis (Figure 5). This suggests that brain parenchyma is likely not experiencing chronic hypoxia induced secondarily by the SU/HY treatment which is comparable to patients evaluated in our study who also lacked ischemic changes. GFAP expression may be largely localized to nuclei more directly regulating ANS control downstream of the cerebrum under acute conditions, such as been shown in spontaneously hypertensive rats expressing astroglial GFAP in the rostral ventrolateral medulla of the brainstem preceding increased sympathetic output from the CNS (21,22).

The chemokine family of small proteins are generally involved with inducing immune cell migration into the CNS in addition to facilitating neural development, survival, and synaptic transmission (23,24). CCL3 is more highly expressed in several neuroinflammatory diseases including MS and its mouse model experimental autoimmune encephalomyelitis (EAE) (25,26), closed head injury (27), ischemia (28), Wallerian degeneration (29), Alzheimer's disease (30) and HIV infection (31). In this study, we found CNS derived CCL3 expression was markedly higher in PH rats as evidenced by an increase in number of CNS cells surrounding brain parenchymal arterioles expressing CCL3 (Figure 4). The endothelial component of the BBB as well as the surrounding brain cells including microglia, astrocytes, and infiltrating immune cells are major sources of inflammatory chemokines like CCL3 during neuroinflammation (26,32,33). The pathological consequence of CNS derived CCL3 expression largely depends on the cell type expressing it which was not explored in this study, however, have been studied in other contexts. TNF- α introduced to the BBB may induce CCL3 expression by vascular endothelium and surrounding glial cells (23). Our results showing increased CCL3 could be a result of microglial activation and TNF- α activity, which has been recently evidenced in MCT induced PH

rats which showed microglial activation with increased IL-1 β , IL-6, and TNF- α mRNA transcripts in the PVN (12). Furthermore, glial and endothelial derived CCL3 alone is not sufficient to drive immune cell migration through the BBB under inflammatory conditions induced by TNF- α and IFN- γ in-vitro, however, may increase cell adhesion rather than transmigration of immune cells near the BBB (23,34). This could explain the lack of more severe structural changes in neuropathology in experimental PH and patients with PAH in our study.

Neurovascular changes, neuroinflammation, and cognitive deficits have been characterized in rodent models of diseases considered less severe than PH like atherosclerosis (14). Previously, another study led by Buga et al. carried out the similar experiments on atherosclerotic mice and found increased brain arteriole wall thickening, perivascular brain parenchymal expression of CCL3, and cognitive deficits. While the present study did not carry out behavioral testing on PH rats, we demonstrate that PH rats exhibited significantly more cells composing perivascular CNS tissue that were expressing CCL3 and increased vascular wall thickening of brain parenchymal arterioles. Similar results presented between these studies provide the first histological evidence for brain changes in PAH which may bring about similar disparities in PAH patients who suffer cognitive impairments, depression, anxiety, and decreased quality of life (4).

It is possible that peripherally derived inflammatory compounds implicated in PAH may affect lung pathology by regulating sympathetic outflow from the CNS. TNF- α , for example, is considered a key inflammatory cytokine in PAH progression (35). Blood TNF- α and IL-6 are elevated in patients and animal models of PH (36–38); and are shown to increase in the PVN of MCT induced PH rats (12). Peripherally administered TNF- α acts on the Subfornical Organ CVO to increase heart rate and blood pressure (39) and induces chemokine expression, like CCL3, in the brain from glia and BBB endothelium to facilitate immune cell trafficking into the CNS (23). IFN- γ elicits a similar response (23) and is also heavily implicated in human PAH (40). Thus,

circulating levels of inflammatory mediators that are enhanced with the progression of PAH may eventually prove to contribute significantly to the overactive sympathetic response observed in PAH patients (2) by their effects on central regulatory systems like CVOs (39), and possibly by their effects on neuroinflammation, a condition which is generally involved with sympathetic overactivity (41).

Peripherally derived vasoactive compounds like Angiotensin-II may also interact with the CNS in addition to contributing to lung pathology in PAH. Circulating Ang-II is responsible for increasing sympathetic outflow via activation of AT1R expressed throughout the brain and particularly in CVOs, and studies have shown that activation of AT1R triggers the release of pro-inflammatory cytokines that participate in neuroinflammation (42,43) in conjunction with heart failure in rats (44) . The beneficial effects of reducing Ang-II activity shown in experimental PH (45) may be in part due to attenuating neuropathology as described in addition to promoting angiogenesis in the brain, as shown in a model for stroke in rats (46). Thus, further exploration of the pathogenesis of PAH through the lens of the lung-brain axis may help identify new targets for treating this devastating disease.

Figure Legends

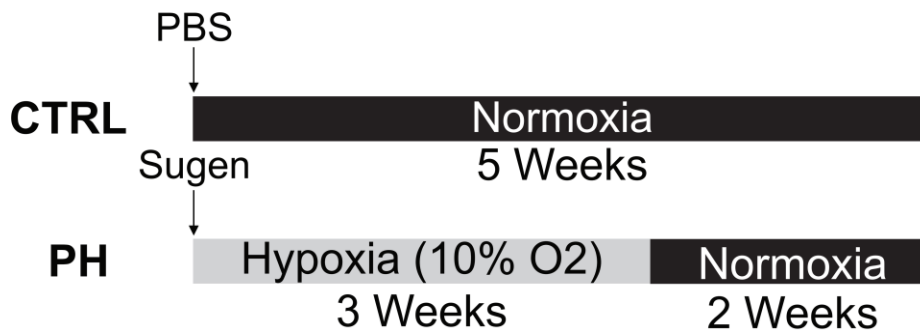


Figure 1. Experimental Protocol. Control rats (CTRL) received phosphate buffered saline (PBS) at day 0 and were followed for 5 weeks. To induce PH, rats in SU/HY group received a single injection of VEGF-R antagonist Sugden as day 0, were kept in hypoxia chamber (10% O₂) for 3 weeks followed by normoxia for 2 weeks.

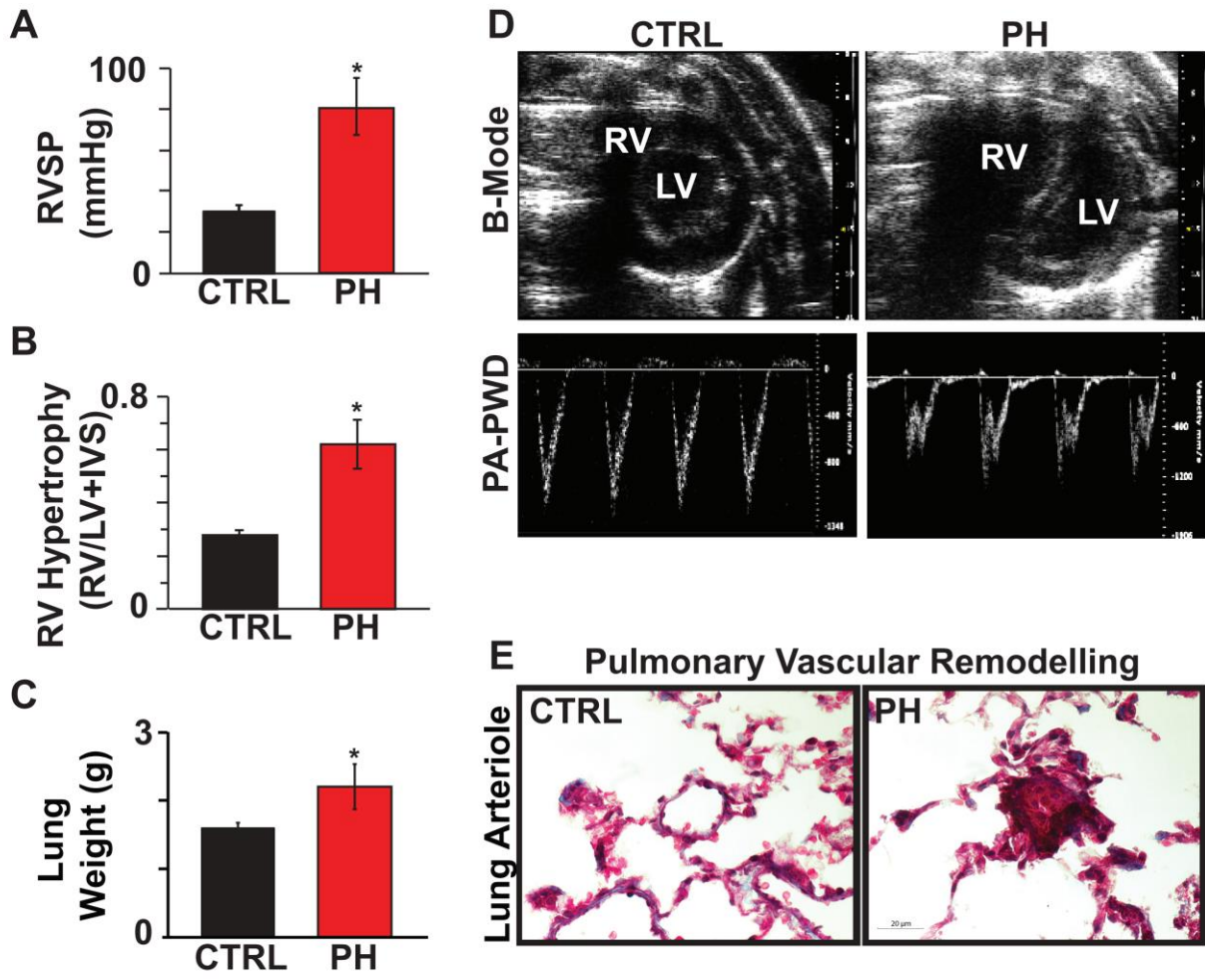


Figure 2. Development of severe angioproliferative PH in rats. Bar graphs showing right ventricular systolic pressure (RVSP, mmHg) (Panel A), right ventricular hypertrophy index (RV/LV+IVS) (Panel B) and lung weight (g) (Panel C) in control (CTRL) and Sugden/hypoxia (SU/HY) groups. Transthoracic echocardiography of rats showing B-mode (Panel D, upper) and pulmonary artery pulsed wave Doppler (PA-PWD) echo images (Panel D, lower). Panel E shows pulmonary arteriolar thickening in SU/HY compared to CTRL. * $p < 0.05$ vs. CTRL; $n = 5$ per group.

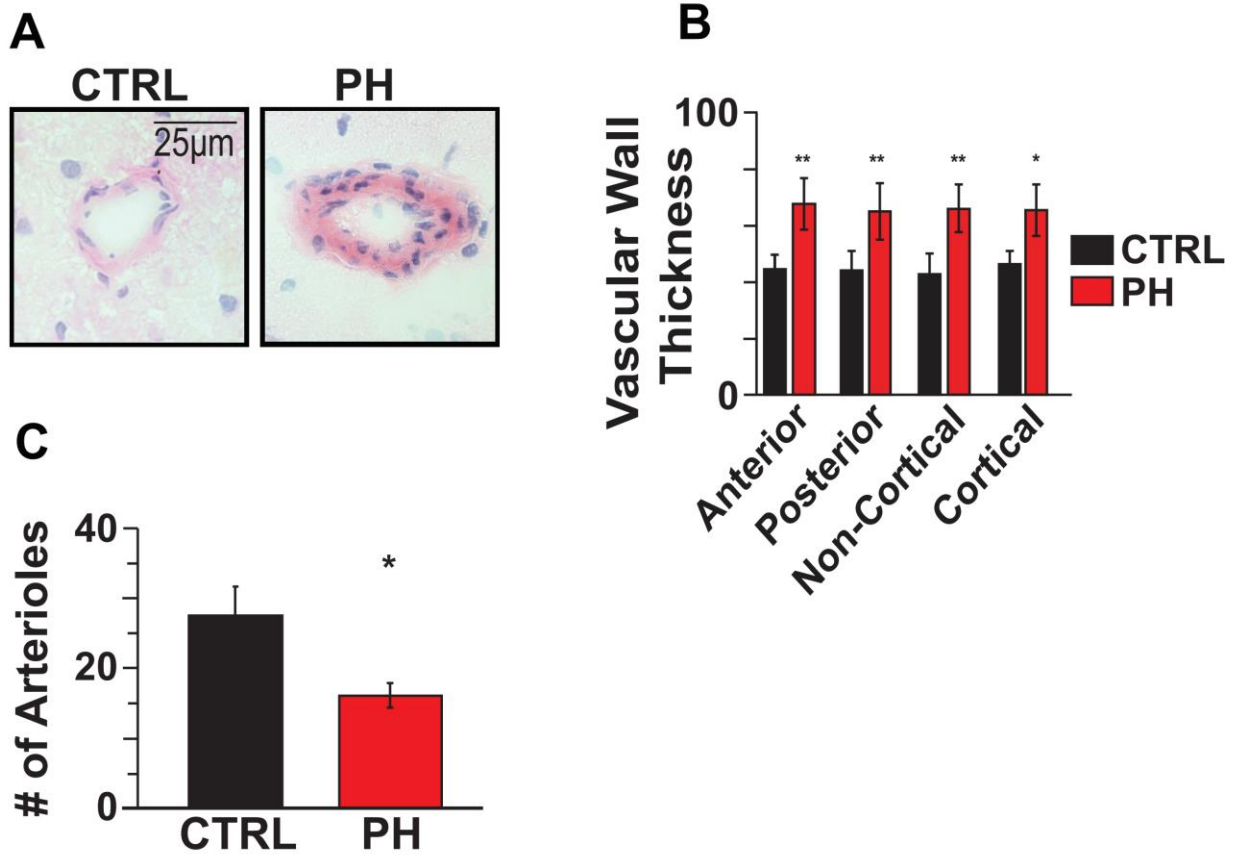


Figure 3. Development of vascular remodeling in brains of rats with PH. A) Representative images of Control and SU/HY rats. B) Bar graphs showing percent wall thickening of blood vessels in Hematoxylin and Eosin stained brain sections of control (CTRL, n=3) and Sugen/hypoxia induced PH (SU/HY induced PH, n=5) groups. * $p < 0.05$ vs. CTRL. C) Numer of brain parenchymal arterioles counted in anterior and posterior combined per group.

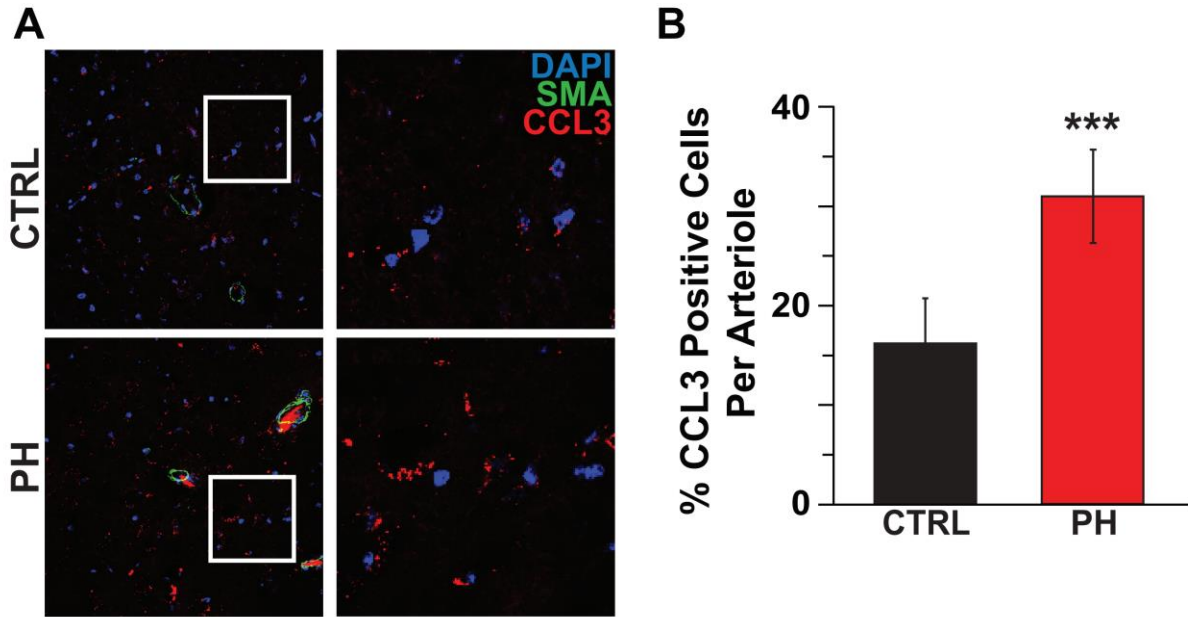


Figure 4. Development of neuro-inflammation in brains of rats with PH. A) Representative images of CCL3 (red) expressed by parenchymal cells in the CNS visualized with nuclear stain DAPI (Blue) and located near vasculature stained with α -SMA (green). B) Bar graphs showing percentage of CNS cells expressing MIP-1 α (CCL3) positive cells compared to control in immunofluorescence-stained brain sections of control (CTRL) and Sugden/hypoxia (SU/HY) groups. *** p <0.001 vs. CTRL; n =5 per group.

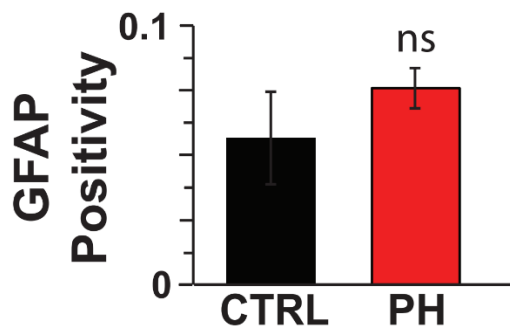


Figure 5. Severe gliosis is not associated with PH in rats. Bar graph showing GFAP expression of reactive astrocytes as measured by positive pixel count algorithm. ^{ns} p >.05 vs CTRL; n =5 per group.

References

1. Lai Y-C, Potoka KC, Champion HC, Mora AL, Gladwin MT. Pulmonary Arterial Hypertension: The Clinical Syndrome. *Circ Res*. 2014 Jun 20;115(1):115–30.
2. Ciarka A, Doan V, Velez-Roa S, Naeije R, van de Borne P. Prognostic Significance of Sympathetic Nervous System Activation in Pulmonary Arterial Hypertension. *Am J Respir Crit Care Med*. 2010 Jun 1;181(11):1269–75.
3. Velez-Roa S, Ciarka A, Najem B, Vachier J-L, Naeije R, Borne P van de. Increased Sympathetic Nerve Activity in Pulmonary Artery Hypertension. *Circulation*. 2004 Sep 7;110(10):1308–12.
4. White J, Hopkins RO, Glissmeyer EW, Kitterman N, Elliott CG. Cognitive, emotional, and quality of life outcomes in patients with pulmonary arterial hypertension. *Respir Res*. 2006;7(1):55.
5. Carson MJ, Doose JM, Melchior B, Schmid CD, Ploix CC. CNS immune privilege: hiding in plain sight. *Immunol Rev*. 2006 Oct;213:48–65.
6. Galea I, Bechmann I, Perry VH. What is immune privilege (not)? *Trends in Immunology*. 2007 Jan 1;28(1):12–8.
7. Dantzer R, O'Connor JC, Freund GG, Johnson RW, Kelley KW. From inflammation to sickness and depression: when the immune system subjugates the brain. *Nat Rev Neurosci*. 2008 Jan;9(1):46–56.
8. Sankowski R, Mader S, Valdés-Ferrer SI. Systemic Inflammation and the Brain: Novel Roles of Genetic, Molecular, and Environmental Cues as Drivers of Neurodegeneration. *Front Cell Neurosci* [Internet]. 2015 Feb 2 [cited 2017 May 28];9. Available from: <http://www.ncbi.nlm.nih.gov/pmc/articles/PMC4313590/>
9. Jerry Yu. Neuroendocrine-Immune Interactions in Lung Inflammatory Diseases [Internet]. *BrainImmune: Trends in Neuroendocrine Immunology*. 2013 [cited 2017 May 28]. Available from: <http://brainimmune.com/neuroendocrine-immune-interactions-in-lung-inflammatory-diseases/>
10. Vaillancourt M, Chia P, Sarji S, Nguyen J, Hoftman N, Ruffenach G, et al. Autonomic nervous system involvement in pulmonary arterial hypertension. *Respir Res*. 2017 Dec 4;18(1):201.
11. Hilzendeger AM, Shenoy V, Raizada MK, Katovich MJ. Neuroinflammation in Pulmonary Hypertension: Concept, Facts and Relevance. *Curr Hypertens Rep*. 2014 Sep;16(9):469.
12. Sharma RK, Oliveira AC, Kim S, Rigatto K, Zubcevic J, Rathinasabapathy A, et al. Involvement of Neuroinflammation in the Pathogenesis of Monocrotaline-Induced Pulmonary Hypertension Novelty and Significance. *Hypertension*. 2018 Jun 1;71(6):1156–63.

13. Gudi V, Gingele S, Skripuletz T, Stangel M. Glial response during cuprizone-induced de- and remyelination in the CNS: lessons learned. *Front Cell Neurosci* [Internet]. 2014 [cited 2017 Apr 30];8. Available from: <http://journal.frontiersin.org/article/10.3389/fncel.2014.00073/full>
14. Buga GM, Frank JS, Mottino GA, Hendizadeh M, Hakhamian A, Tillisch JH, et al. D-4F decreases brain arteriole inflammation and improves cognitive performance in LDL receptor-null mice on a Western diet. *J Lipid Res*. 2006 Oct 1;47(10):2148–60.
15. Sofroniew MV. Molecular dissection of reactive astrogliosis and glial scar formation. *Trends Neurosci*. 2009 Dec;32(12):638–47.
16. Eng LF, Ghirnikar RS. GFAP and astrogliosis. *Brain Pathol*. 1994 Jul;4(3):229–37.
17. Malenfant S, Brassard P, Paquette M, Blanc OL, Chouinard A, Bonnet S, et al. Ventilatory and Cerebrovascular Responses to Hypercapnia in Pulmonary Arterial Hypertension. *FASEB J*. 2016 Apr 1;30(1 Supplement):774.21-774.21.
18. Wang T, Xiao F, Wu G, Fang J, Sun Z, Feng H, et al. Impairments in Brain Perfusion, Metabolites, Functional Connectivity, and Cognition in Severe Asymptomatic Carotid Stenosis Patients: An Integrated MRI Study. *Neural Plast* [Internet]. 2017 [cited 2018 May 19];2017. Available from: <https://www.ncbi.nlm.nih.gov/pmc/articles/PMC5309400/>
19. Purves D, Augustine GJ, Fitzpatrick D, Katz LC, LaMantia A-S, McNamara JO, et al. The Blood Supply of the Brain and Spinal Cord. *Neuroscience* 2nd edition [Internet]. 2001 [cited 2018 Jun 10]; Available from: <https://www.ncbi.nlm.nih.gov/books/NBK11042/>
20. Lee RM. Morphology of cerebral arteries. *Pharmacol Ther*. 1995 Apr;66(1):149–73.
21. Marina N, Ang R, Machhada A, Kasymov V, Karagiannis A, Hosford PS, et al. Brainstem hypoxia contributes to the development of hypertension in the spontaneously hypertensive rat. *Hypertension*. 2015 Apr;65(4):775–83.
22. Turlejski T, Humoud I, Desai R, Smith KJ, Marina N. Immunohistochemical evidence of tissue hypoxia and astrogliosis in the rostral ventrolateral medulla of spontaneously hypertensive rats. *Brain Res*. 2016 Nov 1;1650:178–83.
23. De Laere M, Sousa C, Meena M, Buckinx R, Timmermans J-P, Berneman Z, et al. Increased Transendothelial Transport of CCL3 Is Insufficient to Drive Immune Cell Transmigration through the Blood–Brain Barrier under Inflammatory Conditions In Vitro. *Mediators Inflamm* [Internet]. 2017;2017. Available from: <https://www.ncbi.nlm.nih.gov/pmc/articles/PMC5463143/>
24. Williams JL, Holman DW, Klein RS. Chemokines in the balance: maintenance of homeostasis and protection at CNS barriers. *Front Cell Neurosci* [Internet]. 2014 May 28;8. Available from: <https://www.ncbi.nlm.nih.gov/pmc/articles/PMC4036130/>
25. Simpson JE, Newcombe J, Cuzner ML, Woodroffe MN. Expression of monocyte chemoattractant protein-1 and other beta-chemokines by resident glia and inflammatory cells in multiple sclerosis lesions. *J Neuroimmunol*. 1998 Apr 15;84(2):238–49.

26. Balashov KE, Rottman JB, Weiner HL, Hancock WW. CCR5+ and CXCR3+ T cells are increased in multiple sclerosis and their ligands MIP-1 α and IP-10 are expressed in demyelinating brain lesions. *Proc Natl Acad Sci U S A*. 1999 Jun 8;96(12):6873–8.
27. Israelsson C, Wang Y, Kylberg A, Pick CG, Hoffer BJ, Ebendal T. Closed Head Injury in a Mouse Model Results in Molecular Changes Indicating Inflammatory Responses. *J Neurotrauma*. 2009 Aug;26(8):1307–14.
28. Cowell RM, Xu H, Galasso JM, Silverstein FS. Hypoxic-ischemic injury induces macrophage inflammatory protein-1 α expression in immature rat brain. *Stroke*. 2002 Mar;33(3):795–801.
29. Perrin FE, Lacroix S, Avilés-Trigueros M, David S. Involvement of monocyte chemoattractant protein-1, macrophage inflammatory protein-1 α and interleukin-1 β in Wallerian degeneration. *Brain*. 2005 Apr;128(Pt 4):854–66.
30. Tripathy D, Thirumangalakudi L, Grammas P. Expression of macrophage inflammatory protein 1- α is elevated in Alzheimer's vessels and is regulated by oxidative stress. *J Alzheimers Dis*. 2007 Jul;11(4):447–55.
31. Letendre SL, Lanier ER, McCutchan JA. Cerebrospinal fluid beta chemokine concentrations in neurocognitively impaired individuals infected with human immunodeficiency virus type 1. *J Infect Dis*. 1999 Aug;180(2):310–9.
32. Boven LA, Montagne L, Nottet HSLM, De Groot CJA. Macrophage inflammatory protein-1 α (MIP-1 α), MIP-1 β , and RANTES mRNA semiquantification and protein expression in active demyelinating multiple sclerosis (MS) lesions. *Clin Exp Immunol*. 2000 Nov;122(2):257–63.
33. Ambrosini E, Remoli ME, Giacomini E, Rosicarelli B, Serafini B, Lande R, et al. Astrocytes Produce Dendritic Cell-Attracting Chemokines In Vitro and in Multiple Sclerosis Lesions. *J Neuropathol Exp Neurol*. 2005 Aug 1;64(8):706–15.
34. Lopez-Ramirez MA, Male DK, Wang C, Sharrack B, Wu D, Romero IA. Cytokine-induced changes in the gene expression profile of a human cerebral microvascular endothelial cell-line, hCMEC/D3. *Fluids Barriers CNS*. 2013 Sep 19;10:27.
35. Hurst LA, Dunmore BJ, Long L, Crosby A, Al-Lamki R, Deighton J, et al. TNF α drives pulmonary arterial hypertension by suppressing the BMP type-II receptor and altering NOTCH signalling. *Nature Communications*. 2017 Jan 13;8:14079.
36. Steiner MK, Syrkina OL, Kolliputi N, Mark EJ, Hales CA, Waxman AB. IL-6 Overexpression Induces Pulmonary Hypertension. *Circ Res*. 2009 Jan 30;104(2):236–44.
37. Fujita M, Shannon JM, Irvin CG, Fagan KA, Cool C, Augustin A, et al. Overexpression of tumor necrosis factor- α produces an increase in lung volumes and pulmonary hypertension. *American Journal of Physiology-Lung Cellular and Molecular Physiology*. 2001 Jan 1;280(1):L39–49.

38. Tamosiuniene R, Tian W, Dhillon G, Wang L, Sung YK, Gera L, et al. Regulatory T cells limit vascular endothelial injury and prevent pulmonary hypertension. *Circ Res*. 2011 Sep 30;109(8):867–79.
39. Wei S-G, Zhang Z-H, Beltz TG, Yu Y, Johnson AK, Felder RB. Subfornical Organ Mediates Sympathetic and Hemodynamic Responses to Blood-borne Pro-Inflammatory Cytokines. *Hypertension*. 2013 Jul;62(1):118–25.
40. George PM, Oliver E, Dorfmueller P, Dubois OD, Reed DM, Kirkby NS, et al. Evidence for the involvement of type I interferon in pulmonary arterial hypertension. *Circ Res*. 2014 Feb 14;114(4):677–88.
41. Haspula D, Clark MA. Neuroinflammation and sympathetic overactivity: Mechanisms and implications in hypertension. *Autonomic Neuroscience: Basic and Clinical*. 2018 Mar 1;210:10–7.
42. Platten M, Youssef S, Hur EM, Ho PP, Han MH, Lanz TV, et al. Blocking angiotensin-converting enzyme induces potent regulatory T cells and modulates TH1- and TH17-mediated autoimmunity. *Proc Natl Acad Sci USA*. 2009 Sep 1;106(35):14948–53.
43. Kettenmann H, Hanisch U-K, Noda M, Verkhratsky A. Physiology of Microglia. *Physiological Reviews*. 2011 Apr 1;91(2):461–553.
44. Yu Y, Wei S-G, Weiss RM, Felder RB. Angiotensin II Type 1a Receptors in the Subfornical Organ Modulate Neuroinflammation in the Hypothalamic Paraventricular Nucleus in Heart Failure Rats. *Neuroscience*. 2018 Jun 15;381:46–58.
45. De Man F, Tu L, Handoko L, Rain S, Ruitter G, François C, et al. Dysregulated renin-angiotensin-aldosterone system contributes to pulmonary arterial hypertension. *Am J Respir Crit Care Med*. 2012 Oct;186(8):780–9.
46. Guan W, Somanath PR, Kozak A, Goc A, El-Remessy AB, Ergul A, et al. Vascular Protection by Angiotensin Receptor Antagonism Involves Differential VEGF Expression in Both Hemispheres after Experimental Stroke. *PLOS ONE*. 2011 Sep 1;6(9):e24551.